

## Erratum: Spatiotemporal dynamics and plastic flow of vortices in superconductors with periodic arrays of pinning sites [Phys. Rev. B 54, 16 108 (1996)]

C. Reichhardt, J. Groth, C. J. Olson, Stuart B. Field, and Franco Nori

[S0163-1829(97)06234-6]

Due to poor contrast in the original publication, Figs. 3 and 4 are reproduced below to better illustrate the author's discussion. Further related information, including videos, is available at the following URL:

[http://www-personal.engin.umich.edu/~nori/paps/paps\\_index.html](http://www-personal.engin.umich.edu/~nori/paps/paps_index.html)

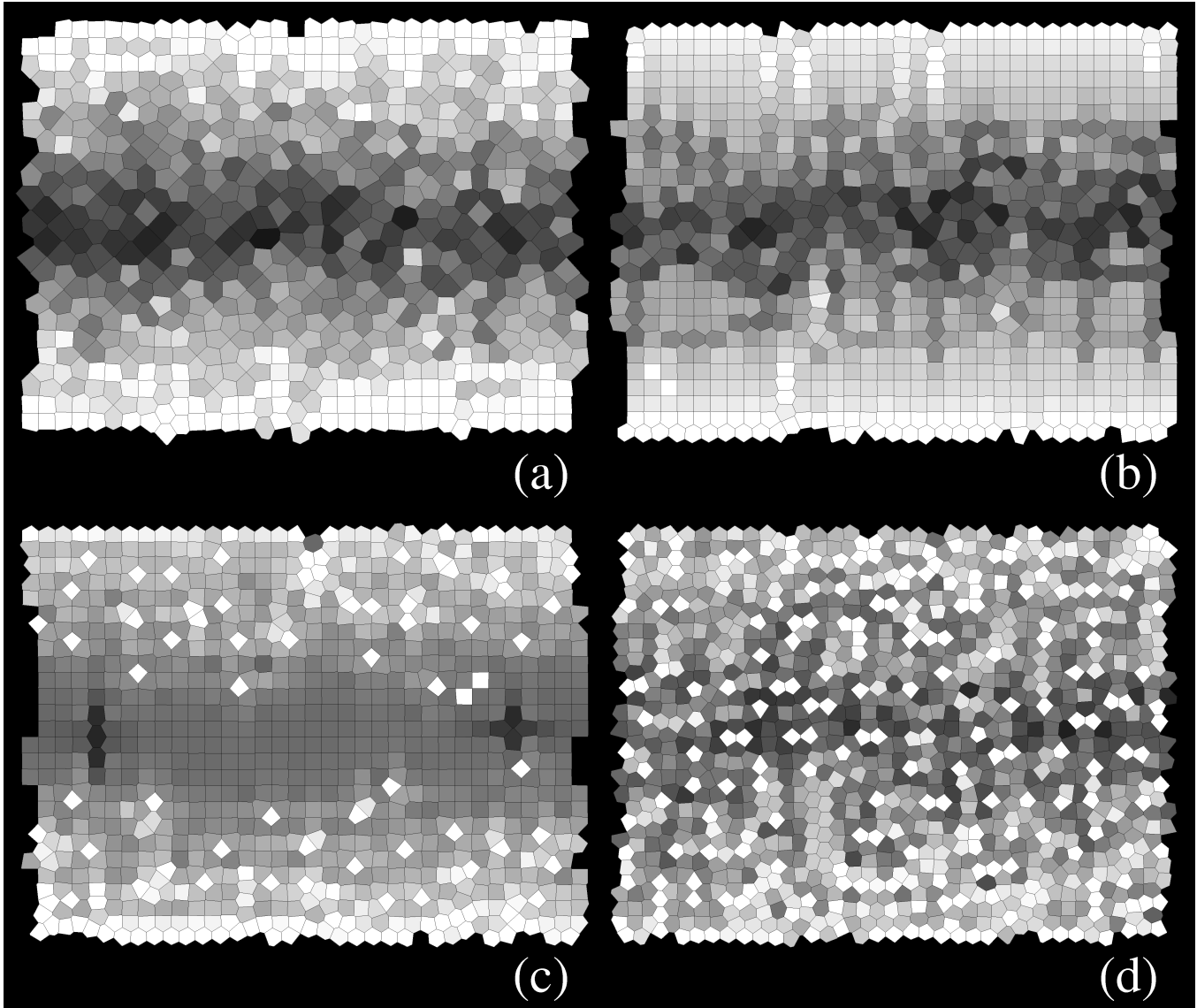


FIG. 3. (a)–(d) Voronoi (Wigner-Seitz) cell construction indicating the location of the vortices as they move through the first matching peak  $n_v/n_p \approx 1$ , for the square PAPS system described in Fig. 1(a). Larger (smaller) cells correspond to low (high) densities of flux lines and are indicated in dark (light) shading. The sample has periodic boundary conditions on the left and right sides, and the vortices penetrate at the top and bottom edges of the sample. (a)–(d) correspond to locations on  $M(H)$  indicated in Fig. 1(a) by the letters  $a$ – $d$ . Before the matching peak  $n_v/n_p \approx 1$  [frame (a)] and right at the matching peak [frame (b)], the PAPS and the VL are commensurate only near the edges of the sample, as indicated by the squares. (b) At the peak in  $M(H)$ , 1D *stringlike defects* which are perpendicular to the edges (or along  $60^\circ$  angles for the triangular case) originate from the boundaries. These gradually destroy the commensurability between the PAPS and the VL at the sample edges, shifting it towards the center of the sample [in (c)] when  $H$  is increased. In (c), just past the peak in  $M(H)$ , the smallest (white) diamond-shaped cells (which look like squares rotated  $45^\circ$  from the horizontal) are mobile interstitial vortices whose plastic flow destroys the commensurability. These are also clearly present in (d), further down in  $M(H)$ , where commensurability effects disappear. This loss of commensurability can be quantified by observing in Fig. 1(c) the drastic drop in  $P_4$  right after the commensurate peak.

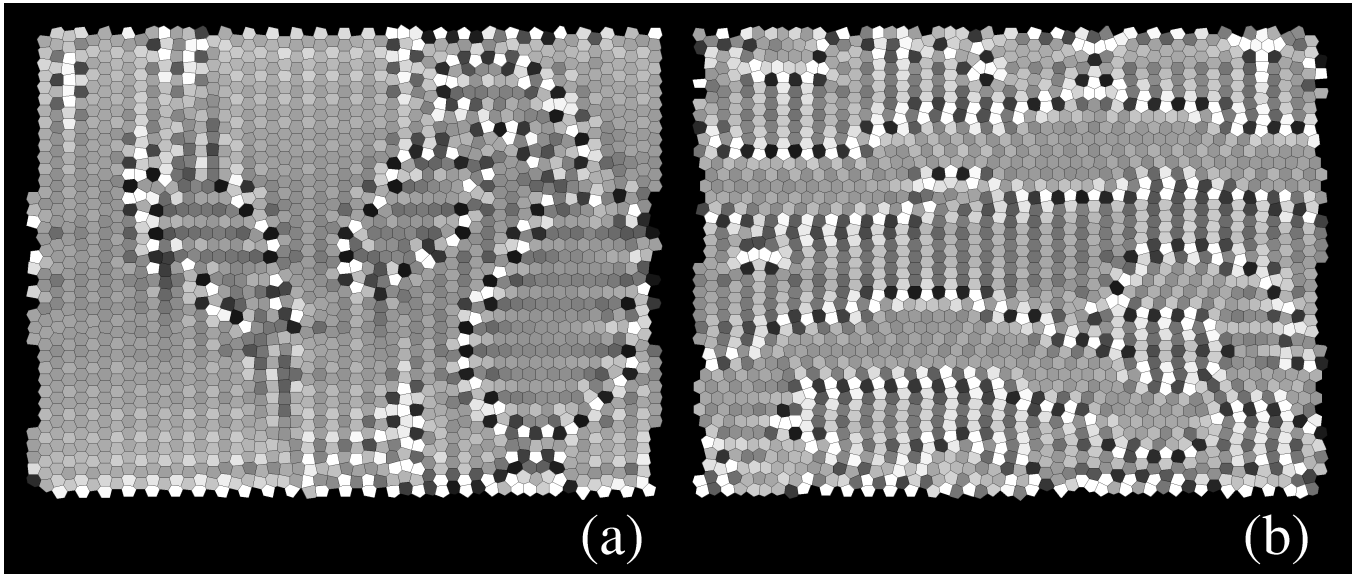


FIG. 4. Vortex configurations for a square PAPS with a lower density of pins of higher strength:  $n_p = 0.49/\lambda^2$ ,  $f_p = 1.4f_0$ ,  $\xi_p = 0.25\lambda$ ,  $N_p = 4.75$ , at (a)  $H = 2.1\Phi_0/\lambda^2$  and (b)  $H = 2.2\Phi_0/\lambda^2$ . Vortex arrangements of different orientations form complex domains of various shapes including (a) islands and (b) stripes, both surrounded by *current-carrying winding strings* of five to seven disclination pairs. These unexpected and striking flux domain patterns continuously evolve as a function of the applied field. These results show that, in general, the current distribution is *not* terraced. This is in contrast to predictions by static 1D models. We also note that the islands and stripes of (approximately) constant  $B$ , surrounded by curved domain boundaries carrying large currents, contain weak currents because in them  $\nabla \times \mathbf{B} \approx 0$ .